Distorted amides as models for activated peptide NC:O units produced during enzyme-catalyzed acyl transfer reactions. 1. The mechanism of hydrolysis of 3,4-dihydro-2-oxo-1,4-ethano...

ARTICLE *in* THE JOURNAL OF ORGANIC CHEMISTRY · JULY 1986

Impact Factor: 4.72 · DOI: 10.1021/jo00364a012

2 AUTHORS:

Vishwa Somayaji
University of Alberta
22 PUBLICATIONS **423** CITATIONS
SEE PROFILE

R. Stan Brown
Queen's University
228 PUBLICATIONS **4,512** CITATIONS
SEE PROFILE

Distorted Amides as Models for Activated Peptide N—C=O Units Produced during Enzyme-Catalyzed Acyl Transfer Reactions. 1. The Mechanism of Hydrolysis of 3,4-Dihydro-2-oxo-1,4-ethanoquinoline and 2,3,4,5-Tetrahydro-2-oxo-1,5-ethanobenzazepine

V. Somayaji and R. S. Brown*

Department of Chemistry, University of Alberta, Edmonton, Alberta, Canada, T6G 2G2

Received February 25, 1986

A series of four substituted benzoquinuclidones (6-X-3,4-dihydro-2-oxo-1,4-ethanoquinoline, X = H, CH_3, OCH_3, Cl) (**3a–d**) and the next higher homologue [2,3,4,5-tetrahydro-2-oxo-1,5-ethanobenzazepine (**5**)] were synthesized and their hydrolyses studied. These are considered as models for the putative distorted amide N—C=O unit in the Michaelis complex produced during enzyme-catalyzed hydrolyses of peptides. Compound **3**, with an sp^3-like N having complete orthogonality of the N lone pair and C=O π-bond, hydrolyzes rapidly at all pH values and shows a pH/rate profile consisting of H_2O attack on an N-protonated species, as well as H_2O and OH^- attack on the neutral species. Strong general base catalysis of H_2O attack is observed in the OH^- domain. Acetate and formate give curved buffer plots consistent with superimposed general catalysis in the acid domain. Amide **5**, in which the N is also sp^3 hybridized and the N—C=O dihedral angle is 30–35°, shows a pH/rate profile consisting of H_2O attack on an O-protonated species and OH^- attack on the neutral with a minimum at pH 7.0; no H_2O attack on the neutral is observed and general base catalysis is not observed in the OH^- domain. However, buffer catalysis is observed for **5** at pH values <7. ^{18}O-exchange experiments show that in $Na^{18}OH/H_2{}^{18}O$, **3** and **5** produce carboxylates containing only one ^{18}O, indicating that the tetrahedral intermediates are not reversibly produced in base. Also, 50% ^{18}O-enriched **5**, when partially hydrolyzed at pH 10.1 and recovered, shows no loss of ^{18}O. However, in the acid domain, recovered ^{18}O-enriched amide when hydrolyzed in $H_2{}^{16}O$ is shown to incorporate ^{16}O for both **3** and **5** such that the tetrahedral intermediate is formed reversibly for both amides. The ^{18}O-exchange results are discussed in terms of the Deslongchamps' stereoelectronic theory.

The high stability of the amide linkage toward hydrolysis is of crucial importance to biological systems since it allows the construction of robust biopolymers (peptides) from relatively simple amino acid precursors. Nevertheless, Nature has endowed living systems with a series of hydrolytic enzymes (peptidases) which are capable of cleaving the N—C=O linkage extremely rapidly. While the exact mechanism of action of none of these peptidases is known,[1] it seems an attractive hypothesis that a share of the exothermicity of substrate binding is utilized in a productive way by the enzyme to destabilize and thereby activate the scissile substrate bond as the transition state for the acyl transfer reaction is approached.[2]

Studies of amide hydrolyses under drastic conditions of elevated temperature and high[3] or low[3d,e,4] pH are well documented, but cases in which an amide hydrolyses under milder conditions approaching physiological ones are conspicuously sparce. The latter category, for the most part, contains species such as **1**[5] or **2**,[6] which although not distorted, are activated *electronically* toward nucleophilic attack and expulsion of the leaving amino group. Bicyclic

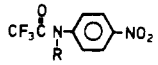

1

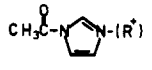

2

amides such as **3a** and **4**, which are torsionally distorted in that the normal amide $^+N{=}C{-}O^-$ resonance is obviated, are reported to be very prone to hydrolysis[7] and methanolysis,[8] respectively. In pioneering studies, Blackburn and co-workers[7,9] have established that both

(1) Walsh, C. *Enzymatic Reduction Mechanisms*; W.H. Freeman: San Francisco, 1979; pp 24–107.

(2) (a) Jencks, W. P. *Adv. Enzymol.* **1975**, *43*, 219–410; (b) **1980**, *51*, 75–106. (c) Bruice, T. C. In *The Enzymes*; Boyer, P. D., Ed.; Academic: New York, 1970; Vol. II, pp 217–279. (d) Fersht, A. *Enzyme Structure and Mechanism*; W. H. Freeman: San Francisco, 1977; pp 226–273. Fersht, A. *Enzyme Structure and Mechanism*, 2nd ed.; W. H. Freeman: San Francisco, 1985; pp 311–346. (e) Jencks, W. P. *Catalysis in Chemistry and Enzymology*; McGraw-Hill: New York, 1969. (f) Wolfenden, R. *Acc. Chem. Res.* **1972**, *5*, 10–18. (g) Haldane, J. B. S. *Enzymes*; Longmans, Green and Co.: London, 1930. (h) Lumry, R. *The Enzymes*; Boyer, P. D., Ed.; Academic: New York, 1959; Vol. I, pp 157–258.

(3) (a) Young, J. K.; Pazhanisamy, S.; Schowen, R. L. *J. Org. Chem.* **1984**, *49*, 4148–4152. (b) Pollack, R. M.; Bender, M. L. *J. Am. Chem. Soc.* **1970**, *92*, 7190–7194. (c) Bender, M. L.; Thomas, R. J. *Ibid.* **1961**, *83*, 4183–4189. (d) Bender, M. L. *Chem. Rev.* **1960**, *60*, 53 and references therein. (e) O'Connor, C. O. *Q. Rev. Chem. Soc.* **1970**, *24*, 553–564 and references therein. (f) Menger, F. M.; Donohue, J. A. *J. Am. Chem. Soc.* **1973**, *95*, 432–438. (g) Kershner, L. D.; Schowen, R. L. *Ibid.* **1971**, *93*, 2014–2024. (h) Schowen, R. L.; Jayaraman, H.; Kershner, L.; Zuorick, G. W. *Ibid.* **1966**, *88*, 4008–4012. (i) Schowen, R. L.; Jayaraman, H.; Kershner, L. *Ibid.* **1966**, *88*, 3373–3375. (j) Drake, D.; Schowen, R. L.; Jayaraman, H. *Ibid.* **1973**, *95*, 454–458. (k) Deslongchamps, P.; Barlet, R.; Taillefer, R. J. *Can. J. Chem.* **1980**, *58*, 2167–2172. (l) Eriksson, S. O.; Bratt, L. *Acta Chem. Scand.* **1967**, *21*, 1812–1822. (m) Bunton, C. A.; Nayak, B.; O'Connor, C. J. *J. Org. Chem.* **1968**, *33*, 572–575. (n) Bender, M. L.; Ginger, R. D.; Kemp, K. C. *J. Am. Chem. Soc.* **1954**, *76*, 3350–3351. (o) Bender, M. L.; Ginger, R. D. *Ibid.* **1955**, *77*, 348–351. (p) Beichler, S. S.; Taft, R. W. *Ibid.* **1957**, *79*, 4927–4935.

(4) (a) Smith, C. R.; Yates, K. *J. Am. Chem. Soc.* **1972**, *94*, 8811–8817. (b) Modro, T. A.; Yates, K.; Beaufays, F. *Can. J. Chem.* **1977**, *55*, 3050–3057. (c) Bunton, C. A.; Farber, S. J.; Milbank, A. J. G.; O'Connor, C. J.; Turney, T. A. *J. Chem. Soc., Perkin Trans. 2* **1972**, 1869–1875. (d) McClelland, R. A. *J. Am. Chem. Soc.* **1975**, *97*, 5281–5282. (e) Bunton, C. A.; O'Connor, C. J.; Turney, T. A. *Chem. Ind. (London)* **1967**, 1835. (f) Williams, A. *J. Am. Chem. Soc.* **1976**, *98*, 5645–5651. (g) Kresge, A. J.; Fitzgerald, P. H.; Chiang, Y. *Ibid.* **1974**, *96*, 4698–4699.

(5) (a) Komiyama, M.; Bender, M. L. *J. Am. Chem. Soc.* **1978**, *100*, 5977–5978; (b) *Bioorg. Chem.* **1978**, *7*, 133–139. (c) Shaskus, J.; Haake, P. *J. Org. Chem.* **1983**, *48*, 2036–2038 and references therein. (d) Pollack, R. M.; Dumsha, T. C. *J. Am. Chem. Soc.* **1975**, *97*, 377–380.

(6) (a) Oakenfull, D. G.; Jencks, W. P. *J. Am. Chem. Soc.* **1971**, *93*, 178–188. (b) Oakenfull, D. G.; Salvesen, K.; Jencks, W. P. *Ibid.* **1971**, *93*, 188–194. (c) Jencks, W. P.; Carriuolo, J. *J. Biol. Chem.* **1959**, *239*, 1272–1279, 1280–1285. (d) Gopalakrishnan, G.; Hogg, J. L. *J. Org. Chem.* **1983**, *48*, 2038–2043 and references therein. (e) Gour-Salin, B. J. *Can. J. Chem.* **1983**, *61*, 2059–2061. (f) Wolfenden, R.; Jencks, W. P. *J. Am. Chem. Soc.* **1961**, *83*, 4390–4393.

(7) Blackburn, G. M.; Skaife, C. J.; Kay, I. T. *J. Chem. Res., Miniprint* **1980**, 3650–3669.

(8) (a) Pracejus, H. von; Kehlen, M.; Kehlen, H.; Matschiner, H. *Tetrahedron* **1965**, *21*, 2257–2270. (b) Pracejus, H. v. *Chem. Ber.* **1959**, *92*, 988–998. (c) Kostyanovskii, R. G.; Mikhlina, E. E.; Levkoeva, E. I.; Yakhontov, L. N. *Org. Mass. Spectrom.* **1970**, *3*, 1023–1029.

(9) (a) Blackburn, G. M.; Plackett, J. D. *J. Chem. Soc., Perkin Trans. 2* **1973**, 981–985; (b) **1972**, 1366–1371.

0022-3263/86/1951-2676$01.50/0

C–N–C(O)–C angle strain[9] and N—C=O torsional strain[7] (for which **3** and **4** could be considered the ultimately strained examples) contribute greatly to the reactivity of amides toward nucleophilic attack. These authors have presented and analyzed a pH vs. log k_{obsd} profile for the hydrolysis of **3a** from pH 5 to 10. They have observed general base catalysis at pH >8 with a Brønsted β of 0.8 but no general catalysis below pH 7.[7] Effects of ring substituents on the hydrolysis were not studied nor were ^{18}O-labeling studies done which would probe the reversible formation of tetrahedral intermediates.

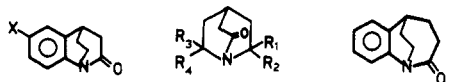

3a X = H
b X = CH_3
c X = OCH_3
d X = Cl

4 **5**

Several questions therefore remain with respect to the course of hydrolysis of this type of strained amide. In this study, we have determined complete pH/rate profiles for **3a–d** in order to delineate the sensitivity of the various kinetic parameters to substituent effects. Secondly, in order to determine how a change in N—C=O dihedral angle from 90° (as in **3**) to ~30–35° influences the hydrolysis, we have synthesized and studied the kinetics of hydrolysis of **5**. Finally, we considered the extent of reversal of formation of the intermediates produced from **3** and **5** in acid and base. The general scheme for base hydrolysis of amides is that in eq 1 wherein reversible addition of OH^- occurs to give a tetrahedral intermediate (T^-). The extent to which T^- partitions to form products

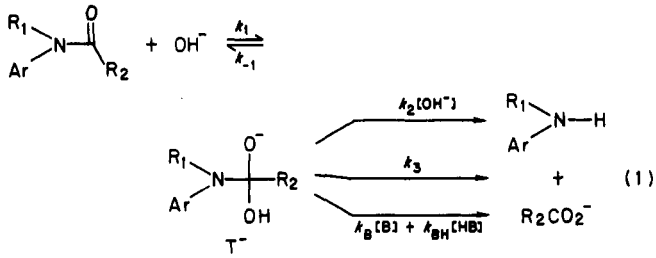

(1)

or starting materials depends on structure, but generally $k_{-1} > (k_2[OH^-] + k_3 + k_B[B] + k_{BH}[BH])$.[10] ^{18}O-labeled primary and secondary benzamides[3m-o] (but not tertiary[3m]) when treated with $NaOH/H_2O$ at elevated temperatures show substantial loss of ^{18}O in the reisolated starting material. In acid hydrolysis, only a miniscule ^{18}O loss is seen in recovered benzamide,[3d] indicating that formation of the tetrahedral intermediate (T^+ in eq 2) is substantially rate limiting. In order to determine the effect of torsional strain on the extent of reversal in both acid and base, we have conducted the hydrolyses of 50% ^{18}O-labeled **3a**, **3c**, and **5** under various conditions.

Experimental Section

a. Materials. Buffers MES (morpholinoethanesulfonic acid), MOPS (morpholinopropanesulfonic acid), HEPES [*N*-(2-hydroxyethyl)piperazine-*N*'-2-ethanesulfonic acid], TRICENE

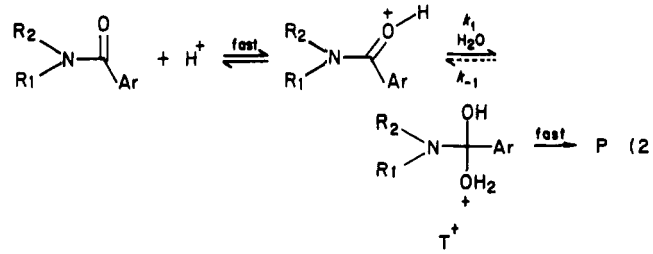

(2)

[*N*-(tris(hydroxymethyl)methyl)glycine], TRIS [tris(hydroxymethyl)aminomethane], BISTRIS [(bis(2-hydroxyethyl)imino)-tris(hydroxymethyl)methane], CHES [2-(cyclohexylamino)-ethanesulfonic acid], and CAPS [3-(cyclohexylamino)propanesulfonic acid] were reagent grade (Sigma). D_2O and $H_2{}^{18}O$ (Merck, Sharp & Dohme Canada) were 99.7% and 97.2% isotopically pure, respectively. Acetonitrile (reagent grade) was purified by double distillation from P_2O_5 and stored over 3-Å molecular sieves. THF was freshly distilled from Na^0 (benzophenone ketyl indicator) under N_2. Benzene, (AnalaR) was freshly distilled from Na^0 prior to use.

Routine ^1H NMR spectra were recorded with a Bruker WP-80 spectrometer, while spectra of the final compounds (**3a–d**, **5**) were recorded with a Bruker WP-200 spectrometer. ^{13}C NMR spectra were recorded at 100.6 MHz with a Bruker WH-400 spectrometer. Routine IR spectra were recorded with a PE Model 297 IR spectrophotometer. Mass spectral analyses were performed with an AEI MS-50 high-resolution mass spectrometer. Negative ion FAB mass spectra (argon impinging on glycerol matrix containing the compound) were recorded with an AEI MS-9 spectrometer locally modified.[12] Mass spectrometric determination of reisolated amide $^{18}O/^{16}O$ ratios were carried out on an AEI MS-12 mass spectrometer.

b. Syntheses. Compounds **3a–d** were prepared by routes analogous to that reported by Blackburn et al.[7] for the preparation of **3a**. The 6-chloro-, 6-methyl-, and 6-methoxy-*N*-(*p*-tolylsulfonyl)-4-oxo-1,2,3,4-tetrahydroquinoline starting materials were prepared by an analogous procedure to that reported for *N*-(tolylsulfonyl)-4-oxo-1,2,3,4-tetrahydroquinoline.[13]

The major modification to the syntheses of **3a–d** related to the conditions utilized for the final synthetic step to construct the bicyclic amide. We found dicyclohexylcarbodiimide (DCC) to be more convenient than the reported[7] closure using triethylamine and ethyl chloroformate.[14] In a typical experiment 1 mmol of 6-X-1,2,3,4-tetrahydroquinoline-4-acetic acid was dissolved in 20 mL of dry acetonitrile followed by 1 mL of a 1.0 M solution of DCC in CH_3CN (1 mmol). The resultant mixture was shaken for a few min to ensure homogeneity and then allowed to stand at room temperature. In 10–20 min, *N,N'*-dicyclohexylurea began to form as white needles. After 4 h, the reaction was essentially complete (as evidenced by IR analysis), at which time the mixture was filtered and the filtrate evaporated under reduced pressure below room temperature to yield a faint yellow oil, isolated yield >90%. Physical characteristics for the final compounds **3a–d** are as follows.

3a: IR (film) 1755 cm^{-1}; ^1H NMR ($CDCl_3$) δ 7.35 (m, 4 H), 3.5 (m, 1 H), 3.41 (m, 1 H), 3.12 (m, 1 H), 2.55 (m, 2 H), 2.00 (m, 1 H), 1.75 (m, 1 H); mass spectrum, *m/z* 173.0839 (calcd for $C_{11}H_{11}NO$, 173.0840).

3b: IR (film) 1750 cm^{-1}; ^1H NMR ($CDCl_3$) δ 7.20 (m, 3 H), 3.48 (m, 1 H), 3.40 (m, 1 H), 3.15 (m, 1 H), 2.50 (m, 2 H), 2.25 (s, 3 H), 1.95 (m, 1 H), 1.70 (m, 1 H); mass spectrum, *m/z* 187.0997 (calcd for $C_{12}H_{13}NO$, 187.0998).

3c: IR (film) 1752 cm^{-1}; ^1H NMR ($CDCl_3$) δ 7.10 (m, 3 H), 3.80 (s, 3 H), 3.45 (m, 1 H), 3.10 (m, 1 H), 2.50 (m, 2 H), 1.90 (m, 1 H), 1.70 (m, 1 H); mass spectrum, *m/z* 203.0950 (calcd for $C_{12}H_{13}NO_2$, 203.0947).

3d: IR (film) 1755 cm^{-1}; ^1H NMR ($CDCl_3$) δ 7.35 (m, 3 H), 3.60 (m, 1 H), 3.42 (m, 1 H), 3.12 (m, 1 H), 2.55 (m, 2 H), 2.05 (m, 1

(10) (a) For the acyl-activated amide such as $CF_3CON(CH_3)C_6H_5$, the observation of nonlinear plots of [buffer] vs. k_{obsd} is interpretable in terms of a change in mechanism whereby at high [buffer] the rate-limiting step becomes $k_1[OH^-]$.[3i,11] (b) For additional example of this phenomenon in the hydrolysis of N-substituted 2,3-dimethylmaleamic acids, see: Aldersley, M. F.; Kirby, A. J.; Lancaster, P. W.; McDonald, R. S.; Smith, C. R. *J. Chem. Soc., Perkin Trans. 2* **1974**, 1487–1495. Kluger, R.; Chin, J.; Choy, W.-W. *J. Am. Chem. Soc.* **1979**, *101*, 6976–6980.

(11) (a) Mader, P. M. *J. Am. Chem. Soc.* **1965**, *87*, 3191–3195. (b) Eriksson, S. O. *Acta Chem. Scand.* **1968**, *22*, 892–906.

(12) Modified by Dr. A. Hogg, Department of Chemistry, University of Alberta.

(13) Johnson, W. S.; Woroch, E. L.; Buell, B. G. *J. Am. Chem. Soc.* **1949**, *71*, 1901–1905.

(14) Denzer, M.; Ott, M. *J. Org. Chem.* **1969**, *34*, 183–187.

Scheme I

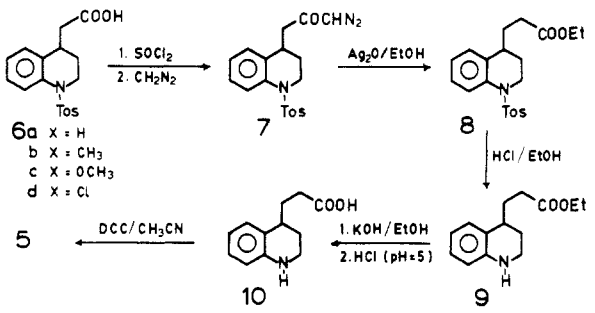

H), 1.80 (m, 1 H); mass spectrum, m/z 207.0462 (calcd for $C_{11}H_{10}NO^{35}Cl$ 207.0459).

2,3,4,5-Tetrahydro-2-oxo-1,5-ethanobenzazepine (5). This was prepared by the sequence given in Scheme I. Ethyl-*N*-(*p*-tolylsulfonyl)-1,2,3,4-tetrahydroquinoline-4-acetic acid (**6**)[7] (3.5 g, 10 mmol) was converted to the corresponding acid chloride by treatment with neat $SOCl_2$ with precautions taken to exclude moisture. After removal of excess $SOCl_2$ under reduced pressure, the residue was dissolved in 25 mL of dry ether and the entire solution cooled to 0 °C. This solution was added slowly to a cooled (0 °C) solution of diazomethane (1.2 g, 30 mmol) in 100 mL of ether with constant swirling. The solution was allowed to come to room temperature for 1 h, after which time the volatiles were removed under reduced pressure.

The crude diazo ketone **7** (IR 2150, 1680 cm^{-1}) was dissolved in 50 mL of ethanol kept at 50–60 °C. A slurry of Ag_2O (1 g) in 10 mL of ethanol was slowly added to the first solution with vigorous stirring over a period of 30 min, after which the mixture was boiled for an additional 30 min, cooled, and filtered. Removal of the volatiles under reduced pressure gave 2.3 g of **8** (58% crude yield from **6**). HCl-catalyzed removal of the *N*-toluenesulfonate group as described[7] yielded 40% of the ester **9**: ^1H NMR ($CDCl_3$) δ 7.0 (m, 2 H), 6.60 (m, 2 H), 4.15 (g, 2 H), 3.82 (br s, 1 H), 3.40 (m, 2 H), 2.88 (m, 1 H), 2.45 (m, 2 H), 1.95 (m, 4 H), 1.26 (t, 3 H); mass spectrum, m/z 233.1418 (calcd for $C_{14}H_{19}NO_2$, 233.1417).

1,2,3,4-Tetrahydroquinoline-4-propanoic Acid (10). This was prepared from **9** in a fashion analogous to that described for the lower homologue:[7] IR (film) 3400, 3250, 1720 cm^{-1}; ^1H NMR ($CDCl_3$) δ 7.15 (br s, 2 H), 7.00 (m, 2 H); 6.55 (m, 2 H), 3.25 (m, 2 H), 2.90 (m, 1 H), 2.50 (m, 2 H), 1.95 (m, 4 H); mass spectrum, m/z 205.1103 (calcd for $C_{12}H_{15}NO_2$, 205.1103).

2,3,4,5-Tetrahydro-2-oxo-1,5-ethanobenzazepine (5). Amide **5** was synthesized from **10** by treatment with DCC in the fashion described above for the general synthesis of **3**: IR (film) 1705 cm^{-1}; ^1H NMR ($CDCl_3$) δ 7.35 (m, 4 H), 4.01 (m, 2 H), 3.34 (m, 2 H), 2.63 (m, 2 H), 2.00 (m, 2 H), 1.85 (m, 2 H), 2.05 (m, 1 H), 1.65 (m, 2 H); mass spectrum, m/z 187.0999 (calcd for $C_{12}H_{13}NO$, 187.0998).

c. Kinetics. Kinetic data were obtained by observing the rate of increase in absorbance of 3×10^{-4} M aqueous solutions of amide at the wavelength of maximum change (290 nm, **3a**; 297 nm, **3b**; 306 nm, **3c**; 302 nm, **3d**; 291 nm, **5**) with a Cary 210 UV–vis spectrophotometer interfaced as previously described.[15] Buffer solutions of four to five concentrations between 0.02 and 0.15 M were used (HCl, pH <2; formate, pH 3.1–4.0; acetate, pH 4.0–5.1; MES, pH 5.1–6.5, MOPS, pH 6.5–7.6; HEPES, pH 7.0–8.1; TRICENE, pH 8.0–8.7; CHES, pH 9.0–9.8; CAPS, pH 9.8–11.1; NaOH, pH >11.0). Stock solutions of amide in CH_3CN were prepared and the reactions initiated by injecting 10 μl of the stock into a 1.0-cm quartz cuvette containing 3.0 mL of buffer solution which had been previously equilibrated in the instrument cell holder for 20 min at 25.0 ± 0.2 °C. All reactions were followed to at least 3 half-lives and displayed excellent pseudo-first-order kinetics. Pseudo-first-order rate constants (k_{obsd}) were obtained by nonlinear least-squares fitting of the absorbance vs. time data to a standard exponential model.[15]

Each determination was repeated in triplicate and has a precision of better than 3%. Data shown in the figures were obtained from plots of k_{obsd} vs. [buffer] at a given pH, the reported values being those extrapolated to zero ionic strength and [buffer]. For the studies to determine curvature in the [buffer] vs. k_{obsd} plots, acetate buffers at pH 5.10 and 4.50 were made up to varying concentrations, the ionic strength being held constant at 0.4 M with KCl. Tables of primary k_{obsd} data are given as supplementary material.

Data for faster reactions ($k_{obsd} > 0.1$ s^{-1}) were obtained with a Durrum–Gibson 115 stopped-flow kinetics system interfaced to a microcomputer.[15] Values reported are the averages of four to eight separate determinations and have a precision of better than 3%. Into one drive syringe was placed the main buffer solution (0.05–0.80 M), while the second syringe contained 5 mL of a very dilute ($\sim 10^{-3}$ M HEPES) buffer held at pH ~8, (corresponding to the conditions of slowest hydrolysis for the amide). Both solutions were thermostated at 25.0 °C for 20 min, after which time 20–30 μL of stock solution of amide in CH_3CN was injected into the dilute buffer. Kinetic determinations were immediately commenced, the amides **3a–d** lasting long enough under these conditions to allow four runs. If necessary, the entire procedure was repeated, to record additional readings. The pH of the effluent was measured and taken to be that of the reaction medium, assuming instant equilibration.

In general, pH measurements during preparation of the aqueous buffers were made with a Fisher 825 MP meter using separate Fisher glass and calomel electrodes. pH measurements of the reaction mixtures after a kinetic run were made with a Radiometer TTT2 unit and Radiometer GK-2321C combination electrode and showed no change during the course of reaction. Electrodes were standardized with certified pH 4.00, 7.00, and 10.00 buffers prior to use.

Deuterated buffers were prepared either by dissolving HCO_2H (pD 3.1) or HEPES (pD 8.0) in 99.7% D_2O (to a final concentration of 0.1 M) and adjusting the pD with NaOD (prepared by addition of Na^0 to D_2O). The addition of this amount of HCO_2H alters the deuterium content by ~0.1% and was assumed not to influence the results. pD was determined by adding 0.4 unit[16] to the readings obtained with the above devices.

Energies of activation were determined graphically from plots of log k_{obsd} vs. $1/T$ at three to four different temperatures.

d. ^{18}O-Exchange Studies. 1. Qualitative Mass Spectral Analysis. Amides **3a–d** and **5** (~5 mg) were dissolved in a solution consisting of 5 μL of CH_3CN and 5 μL of $H_2{}^{18}O$. A small amount of this solution was injected directly into the mass spectrometer at various time intervals and the spectrum recorded for both the amide and carboxylic acid regions. The procedure was repeated until hydrolysis was complete. For ^{18}O-exchange experiments at pH <1, ~5 μL of $H_2{}^{18}O$ (through which dry HCl gas had been passed) was added to a small amount of solid amide. The mass spectrum was again recorded by direct injection of the solution into the spectrometer. For the negative-ion FAB experiments, 5 mg of amide was dissolved in 10 μL of $Na^{18}OH/H_2{}^{18}O$ (pH >12) and a small droplet of this mixed with glycerol and injected into the chamber. For the latter two sets of determinations, only the carboxylic acid was monitored for incorporation since the reaction is very fast. Control experiments were conducted under all the above conditions to determine if the authentic carboxylic acid exchanged; this only occurred under strongly acidic conditions.

2. Quantitative ^{18}O Mass Spectral Analysis. For these experiments 50% ^{18}O-incorporated amide was synthesized and subjected to hydrolysis under conditions nearly identical with those used for the kinetic experiments. Unreacted amide was reisolated after about 1 and 2 half-lives and subjected to mass spectrometric analysis. Percent ^{18}O content for all subsequent experiments is determined as $(I_{M+2})/(I_{M+2} + I_M)$ where I = intensity and M + 2 and M are the ^{18}O and ^{16}O parent peaks. Reported values in the tables are averages of four to six determinations for a given experiment.

The following synthesis of ^{18}O-enriched **3a** is representative. To 122 mg of detosylated **6a** (Scheme I) in an oven-dried 5-mL flask fitted with a reflux condensor were added 600 mg of 98% $H_2{}^{18}O$, concentrated HCl (56 mg), and 476 mg of $H_2{}^{16}O$. The solution was heated at 100 °C for 18 h, cooled, brought to pH 5.0

(15) Brown, R. S.; Ulan, J. G. *J. Am. Chem. Soc.* **1983**, *105*, 2382–2388.

(16) Fife, T. H.; Bruice, T. C. *J. Phys. Chem.* **1961**, *65*, 1079.

by the addition of 8 M NaOH (in $H_2{}^{16}O$), and extracted with 3 × 2 mL of CH_2Cl_2. The combined CH_2Cl_2 extracts were diluted with 5 mL of acetonitrile, decolorized with charcoal, and filtered. On removing all volatiles 70 mg (57%) of the ^{18}O-enriched acid was obtained. The enriched acid was cyclized in an acetonitrile solution containing equimolar DCC as described above to quantitatively yield the amide which contained 48.8 ± 0.8% ^{18}O as judged by comparison of the M + 2 and M peaks in the mass spectrum. In a similar fashion were prepared enriched **3c** and **5**.

Reisolation of starting amide must be carried out quite quickly since **3a,c** and **5** hydrolyze rapidly. To retard the rate of hydrolysis of **3a,c** the reaction was performed at 11 °C in a pH 6.5 or 6.8, 0.04 M MOPS buffer containing 10% CH_3CN. Independent kinetic analysis, done as described above, established that $T_{1/2}$ for **3a** under these conditions is 247 s, while $T_{1/2}$ for **3c** is 181 s. The general reisolation procedure is typified by the following experiment for **5**.

A stock solution of 48.0 ± 0.45% ^{18}O-enriched **5** (4.8 mg in 0.2 mL of CH_3CN) was added to 10 mL of rapidly stirred acetate buffer (pH 4.5, 0.10 M) containing 0.8 mL of CH_3CN (for reasons of improved solubility) and thermostated at 25.0 °C. After 680 s (1 half-life) the reaction mixture was quickly poured into 10 mL of freshly distilled CH_2Cl_2 and shaken in a 30-mL separatory funnel and the lower layer run immediately onto anhydrous Na_2SO_4 (10 g). Extraction of the aqueous layer with a second 10-mL portion of CH_2Cl_2 followed by drying of the combined organic layers and solvent removal under reduced pressure (T < 20 °C) yielded ~4 mg of material comprised of unreacted amide and product acid **10**. This was dissolved in ~20 μL of dry CH_3CN and directly analyzed by mass spectrometry. To obtain the results for 2 half-lives, a second experiment was carried out analogously to the above, with the exception that the isolation was commenced at ~1300 s. Rate constants for ^{18}O exchange were determined from the slopes of plots of ln $(I_{M+2})/(I_{M+2} + I_M)$ as a function of time. The data summary for **3a,c** and **5** are presented in Table IV, while primary data are given in Table S5 (supplementary material).

3. ^{13}C-^{18}O NMR Chemical Shift Experiments. For reasons of solubility, the amide (100–200 mg) was dissolved in 0.5 mL of CD_3CN containing $H_2{}^{18}O$ (45–75 μL for **3** and **5**, ~10–20 vol %) and the full proton-decoupled ^{13}C-spectrum obtained at various time intervals. For **3** which hydrolyzes relatively quickly under these conditions, every 500–1000 scans were summed separately (the time being recorded as the midpoint of the number of scans utilized), and the process was repeated until the amide was no longer observed. For **5**, the reaction was very slow, and the spectra were collected at various time intervals over a period of 3 days. The percentage of ^{18}O incorporation in both amide and product acid was judged from the relative peak heights of $^{18}O/^{16}O$ amide and $^{18}O,^{18}O/^{18}O,^{16}O$ acids, respectively. ^{18}O incorporation is evidenced by the appearance of a new peak attributable to an ^{18}O-induced isotope shift of the carbonyl ^{13}C resonance.[17] Control experiments with 50% ^{18}O-incorporated **5** shows that the $^{13}C{=}^{18}O$ resonance of the amide appears 4.3 Hz upfield from the $^{13}C{=}^{16}O$ resonance at 187.6 ppm. The ratio of peak intensity is 49.1/50.9 ($I_{C=^{18}O}/I_{C=^{16}O}$) while the mass spectrometric ratio is 48 ± 0.5/52 ± 0.5.

Results

a. Kinetics. Shown in Figure 1 are the buffer-independent pH vs. log k_{obsd} profiles for **3a** and **5**. The profiles for amides **3b–d** are nearly superimposable on that for **3a** and for reasons of clarity are not illustrated. (The pseudo-first-order rate constant data from which the plots were constructed are available in Tables S1 and S2, supplementary material.) The profiles for **3a–d** each exhibit domains involving H_2O attack on a protonated species and an apparent H_2O attack followed by OH^- attack on the neutral. No terms of higher order than 1 for OH^- attack are seen. The results for **3a** corroborate those given by Blackburn et al.[7] with the notable exception that at high $[H_3O^+]$, the k_{obsd} values here tend to become pH independent. This indicates a relatively high pK_a (3.5–4) for **3**-H^+ and suggests that the site of protonation is N.[18] The profile for **5** consists of two domains requiring H_2O attack

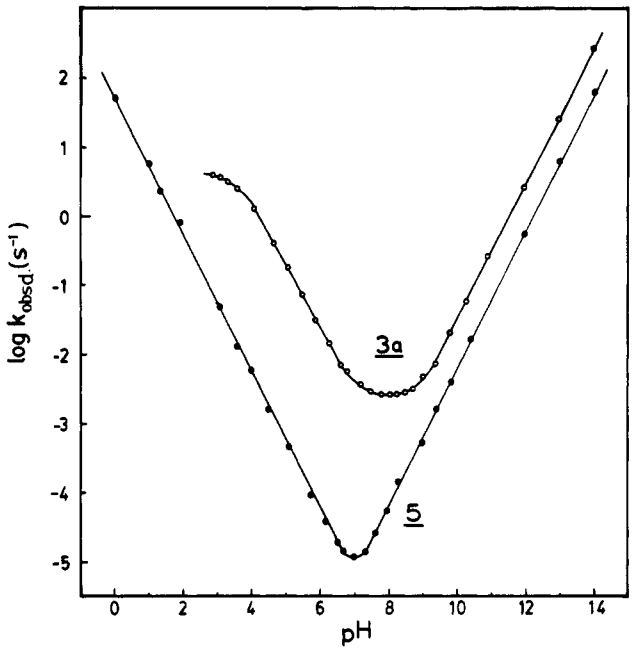

Figure 1. Buffer-independent pH vs. log k_{obsd} profiles for **3a** (○) and **5** (●); T = 25.0 °C.

Table I. Equilibrium and Rate Constant Values for Amides 3a–d and 5 Evaluated by Nonlinear Least-Squares Fitting of Kinetic Data to Equations 3a and 4a, Respectively[a–c]

compound	k_1, s^{-1}	10^3k_2, s^{-1}	$10^{-2}k_{3}$, M^{-1} s^{-1}	$10^{-2}k_{H^+}$, M^{-1} s^{-1}	pK_a
3a	4.4[5]	2.0[2]	2.6[2]		3.7[1]
3b	4.0[5]	1.6[8]	1.7[5]		3.8[1]
3c	5.3[1]	1.6[7]	1.6[8]		3.5[7]
3d	3.5[3]	3.4[2]	3.6[5]		3.3[8]
5			0.6[0]	0.5[9]	

[a] T = 25.0 °C; data extrapolated to [buffer] and ionic strength = 0, [substrate] = 3 × 10^{-4} M. [b] Standard deviation in rate constants 5% and in K_a, 7%. Evaluated by using $K_w = 10^{-14}$. [c] Primary k_{obsd} data at various pH values given in Tables S1 and S2 in supplementary material. [d] $k_{H^+} = k_{H_2O}/K_a{}^{S\text{-}H^+}$.

(17) For leading references to the ^{18}O–^{13}C chemical shift methodology as it pertains to dynamic exchange, see: (a) Parente, J. E.; Risley, J. M.; Van Etten, R. L. *J. Am. Chem. Soc.* **1984**, *106*, 5156–8161. (b) Risley, J. M.; Kuo, F.; Van Etten, R. L. *Ibid.* **1983**, *105*, 1647–1652. (c) Risley, J. M.; Van Etten, R. L.; Uncuta, C.; Balaban, A. T. *Ibid.* **1984**, *106*, 7836–7840. (d) Van Etten, R. L.; Risley, J. M. *Ibid.* **1981**, *103*, 5633–5636. (e) Risley, J. M.; Van Etten, R. L. *Ibid.* **1981**, *103*, 4389–4392. (f) Vederas, J. C. *Ibid.* **1980**, *102*, 374–376. (g) Diakur, J.; Nakashima, T. T.; Vederas, J. C. *Can. J. Chem.* **1980**, *58*, 1311–1315.

(18) Normally simple N-protonated amides have pK_a values of −8 to −6,[19,4f] while O-protonated amides have pK_a values on the order of −2 to 0.[19] The relative acidities can be rationalized on the basis of simple resonance agruments. However, **3** (and to a lesser extent **5**) does not allow such resonance so that the N and carbonyl group should behave as independent amino and ketonic groups but experience mutual inductive effects. Since the pK_a of the C=O$^+$H unit is expected to be even lower than that of a ketone (normally −7.7 to −5 for such ketones as cyclohexanone, acetone, etc.[19c]), the observed kinetic pK_a of ~3.5 for **3a–d** in the present study is attributable to the dissociation of O=CN$^+$H. By way of comparison, the kinetic pK_a of 3.71 for **3a** is some 4.0 units lower than the thermodynamic pK_a reported for benzoquinuclidine (7.79[20]), in line with a significant inductive destabilization by the adjacent C=O unit.

(19) (a) Arnett, E. M. *Prog. Phys. Org. Chem.* **1963**, *1*, 223–403. (b) Guthrie, P. J. *J. Am. Chem. Soc.* **1974**, *96*, 3608–3615. (c) Arnett, E. M.; Quirk, R. P.; Larsen, J. W. *Ibid.* **1970**, *92*, 3977–3984. (d) Fersht, A. *Ibid.* **1971**, *93*, 3504–3515.

(20) Wepster, B. M. *Recl. Trav. Chim. Pays-Bas* **1952**, *71*, 1171–1178.

(21) (a) Jencks, W. P. *Acc. Chem. Res.* **1980**, *13*, 161–169 and references therein; (b) **1976**, *9*, 425–432

Table II. Activation Parameters and Solvent Deuterium Isotope Effects for Hydrolysis of 3c

pH	T, °C	k_{obsd}, s^{-1} [a]	E_a, kcal/mol	$\Delta H^{\ddagger}$, kcal/mol	$\Delta S^{\ddagger}$, eu	k_{H_2O}/k_{D_2O} [b]
8.00[c]	14.1	1.14×10^{-3}	11.0	10.4	−35.9	2.17
	25.0	2.10×10^{-3}				
	37.2	4.51×10^{-3}				
3.2[c]	8.5	1.27	10.8	10.2	−19.8	2.39
	25.0	3.75				
	35.5	6.91				

[a] k_{obsd} values extrapolated to [buffer] = 0; values ±5%. [b] T = 25 °C; pD = pH + 0.4 (Pentz, L.; Thornton, E. R. *J. Am. Chem. Soc.* **1967**, *89*, 6931–6938). [c] pH-independent regions.

on **5**-H^+ and OH^- attack on **5** with a minimum at pH 7 showing no evidence of H_2O attack on the neutral form. Since there is no tendency to plateau at low pH, the pK_a for **5**-H^+ must be <0.

The kinetics for **3** and **5** can most simply be accommodated by the processes given in eq 3 and 4, respectively, where P = product acid, with expressions for the corresponding k_{obsd} values being given in eq 3a and 4a. Non-

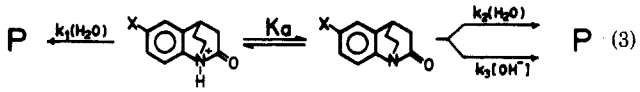

(3)

$$k_{obsd}^{3} = \frac{k_1[H^+]^2 + k_2K_a[H^+] + k_3K_wK_a}{[H^+]^2 + K_a[H^+]} \quad (3a)$$

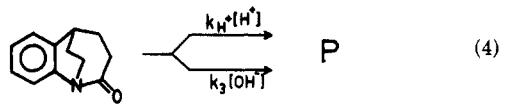

(4)

$$k_{obsd}^{5} = \frac{k_{H^+}[H^+]^2 + k_3K_w}{[H^+]} = k_{H^+}[H^+] + k_3[OH^-] \quad (4a)$$

linear least-squares fitting of the k_{obsd} vs. $[H^+]$ data to the appropriate equation generates the solid curves shown in Figure 1 with the individual constants being given in Table I.

Of all parameters given in Table I, only the k_3 term correlates in a satisfactory way with any Hammett parameter as is shown in Figure 2. With σ, a ρ value of 0.72 ± 0.008 (r = 0.987, four data) is obtained. An equally good line is obtained with σ^- since for these substituents the σ and σ^- constants are the same. The k_2 term adheres to a rough correlation with σ, but the fit is judged to be poorer than for k_3 since it is drastically curved as is illustrated in Figure 2.

Given in Table II are activation parameters and solvent deuterium isotope effects for the hydrolysis of a representative example of **3**, namely **3c**.

b. Buffer Effects. In the pH >8 base domain, buffer catalysis is seen for each of **3a–d**. Two-point Brønsted plots constructed from the data for CAPS and CHES give β values of 0.72, 0.85, 0.75, and 0.67 for **3a–d**, respectively, in agreement with the value of 0.8 ± 0.1 reported by Blackburn et al.[7] for **3a**. Plots of the second-order rate constant for buffer catalysis (k_B) vs. % free base indicate only the basic form is active. With the exception of HEPES and TRICENE, no buffer catalysis is seen between pH 7.5 and 12 for **5**. The former two buffers are particularly active as their basic forms toward **5** and **3a–d** as are other buffering agents containing a basic N and hydroxyalkyl unit. The observed k_B values for HEPES and TRICENE lie well above their expected values estimated for the Brønsted plots defined by CHES and MOPS for **3a–d** and signify a different mechanism of action. Second-order rate constant data for the above buffers are presented as supplementary material in Table S3.

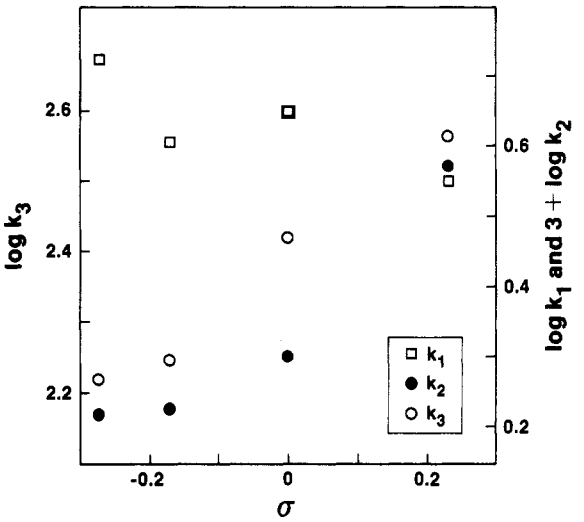

Figure 2. Hammett plots of log k_1 (right scale, □), 3 + log k_2 (right scale, ●), and log k_3 (left scale, ○) against substituent σ values for **3a–d**. Values of rate constants from Table I.

In the neutral and acid domains, the nature of the buffer catalysis for **3** and **5** changes. For example MES gives no observed effect for **3a–d** (pH 5.7–6.5) but does catalyze the hydrolysis of **5**. Plots of k_B vs. % free MES base show that both the acidic and basic forms of the buffer are active. Acetate and formate are also active toward **5**. Plots of k_{obsd} vs. [acetate] at pH 5.1 and 4.5 yield straight lines with slopes of 14.3×10^{-4} and 28.7×10^{-4} M^{-1} s^{-1}, respectively, while similar plots vs. [formate] at pH 4.0 and 3.6 have slopes of 5.76×10^{-2} and 13.2×10^{-2} M^{-1} s^{-1}, respectively.

Acetate and formate at low concentration show quite small and almost unnoticeable effects with **3a–d**, essentially corroborating Blackburn's findings with **3a**. However, at high concentration a trend is discernable, this being most prominent for **3c**. As shown in Figure 3 a saturation behavior exists in the plots of k_{obsd} [total acetate] concentrations at pH 5.1 and 4.5. (Ionic strength was held at 0.4 M, KCl, but changes in ionic strength from 0.1 to 0.4 M do not change the k_{obsd} values more than 3%.) Because the buffer concentrations did not exceed 0.4 M, it is not certain whether the plots eventually become independent of [buffer] or level off at some gradual slope. This type of phenomenon is often seen in multistep reactions wherein a product-forming step proceeding from a reversibly formed intermediate is subject to buffer catalysis.[3j,1,5b,11,21] Data pertaining to the above studies are available in Table S4 (supplementary material).

Imidazole appears to facilitate the decomposition of **3** and **5** by uni- and bimolecular (in [imidazole]) pathways. Plots of K_{obsd} vs. [free imidazole] (pH 7.5, imidazole buffer, T = 25.0 °C) yield upward curving lines which can be analyzed according to eq 5.

$$k_{obsd} = k_{blank} + k_2[Im] + k_3[Im]^2 \quad (5)$$

For **3c** the values for k_{blank}, k_2, and k_3 are 2.25×10^{-3} s^{-1}, 7.75 M^{-1} s^{-1}, and 334 M^{-2} s^{-1}, respectively, while for **5** they

Table III. Fast Atom Bombardment Determined Peak Intensities for Various Amides and Their Product Acids Treated with $Na^{18}OH/H_2{}^{18}O$[a]

compound	time after treatment,[b] min	relative peak intensities, m/z 204	206	208
3b	~15	0	100	2.8
6b[c] (-Tos)	~20	100	2.4	0
5	~5000	0	100	4.9
10[c]	~5000	100	4.2	0

[a] Glycerol matrix containing reaction mixture bombarded with argon. [b] Treatment consists of solid material dissolved in a few microliters of $Na^{18}OH/H_2{}^{18}O$ at room temperature. [c] Product acid as identified in Scheme I.

are 2.60×10^{-5} s^{-1}, 0.019 M^{-1} s^{-1}, and 0.102 M^{-2} s^{-1}.

c. ^{18}O-Labeling Experiments. Given in Table III are fast atom bombardment (FAB) determined masses for product carboxylates formed from treatment of **3b** and **5** with 1 N $Na^{18}OH/H_2{}^{18}O$. It is clear that when the hydrolysis product from a given amide and its authentic nonenriched acid are subjected to as similar conditions as possible and compared, the ratios of the FAB-measured M + 2/M peaks are the same. No evidence of double ^{18}O incorporation is seen within the experimental limitations which we judge to be ±2%. The relatively high value of the error limit stems from the cluttered appearance of the FAB spectra with adventitious glycerol peaks (from the glycerol matrix in which the carboxylates are run) surrounding the parent ions. We believe the clustering is responsible for the anomalously high amount of M + 2 product for **5** and **10** and not the exchange of $H_2{}^{18}O$ into the carboxylate. Control experiments in which the authentic carboxylates are subjected in the $Na^{18}OH/H_2{}^{18}O$ hydrolysis medium and reanalyzed by FAB show that the carboxylates do not incorporate ^{18}O.

Quantitative experiments were conducted as follows. Approximately 50% ^{18}O-enriched amides **3a**, **3c**, and **5** were synthesized as detailed in the Experimental Section and subjected to hydrolysis in a medium consisting of 90% $H_2{}^{16}O$-containing buffer and 10% CH_3CN (for solubility) at temperatures that were convenient for reisolating the amide after various time intervals. The exact conditions and results are given in Table IV with primary data given in Table S5 (supplementary material). Hydrolysis kinetics were monitored in the same buffers under the same conditions of temperature and 10% CH_3CN in order to determine the conditional hydrolytic rate constants reported in Table IV. The pseudo-first-order rate constants for ^{18}O exchange (k_{ex}) were evaluated from the slopes of plots of ln ^{18}O content in recovered amide vs. time. The exchange reactions were followed to two half-times of hydrolysis and the plots displayed excellent linearity.

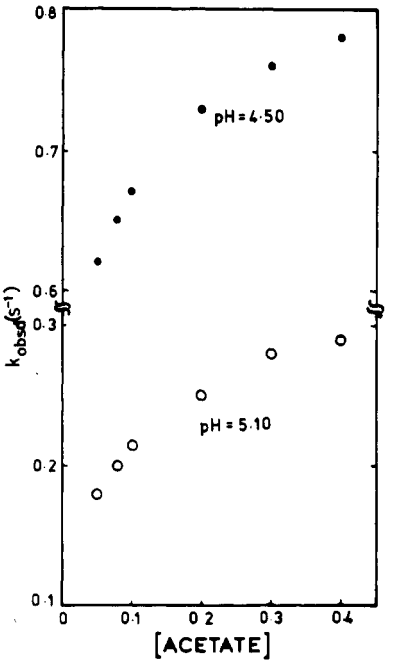

Figure 3. Plots of k_{obsd} vs. total acetate concentration for the hydrolysis of 3×10^{-4} M **3c** at 25 °C in H_2O; μ = 0.4 (KCl).

In the neutral and acid domains for **3a,c** (pH 6.5–6.8) and the acid domain for **5**, large amounts of ^{18}O exchange are observed. However at pH 9.8 where the kinetic profile for **3a** is comprised of both a water term (k_2) and hydroxide term (k_3), a reduced amount of ^{18}O exchange is observed. At pH 10.1, corresponding to the section of the kinetic profile for **5** which is first order in $[OH^-]$, the exchange in recovered amide is (within the experimental error) indistinguishable from zero and confirms the result from FAB.

Finally in Table V we present the exchange data for **3a,c** and **5** determined by $^{18}O{=}{}^{13}C$ NMR chemical shift data obtained in situ from unbuffered CD_3CN solutions containing 10–20 vol % $H_2{}^{18}O$, the exact conditions being given in the table. We assume the "pH" of this medium, although not directly definable is between 7 and 5 since the product amino acid acts as a buffering agent. (Un-

Table IV. Mass Spectrometrically Determined ^{18}O-Exchange Rates of Recovered Amides 3a, 3c, and 5 and Hydrolysis Rate Constants under Various Conditions[a]

compound	pH (buffer) [conc, M]	T, °C	$10^3 k_{hyd}$,[b] s^{-1}	$10^4 k_{ex}$,[c] s^{-1}	k_{ex}/k_{hyd}	% ^{18}O exchange per $T_{1/2}$ hydrolysis
3a	6.5 (MOPS) [0.04]	11.0 ± 0.1	2.80 ± 0.05	8.29 ± 0.7	0.29 ± 0.03	18.4 ± 1.5
3a	9.8 (CHES) [0.02]	11.0 ± 0.1	4.38 ± 0.09	4.65 ± 0.5	0.11 ± 0.014	7.2 ± 0.8
3c[d]	6.8 (MOPS) [0.04]	25.0 ± 0.1	3.82 ± 0.07	8.98[d] ± 1.1	0.24 ± 0.03	15.0 ± 1.9
5	4.5 (acetate) [0.10]	25.0 ± 0.1	1.02 ± 0.02	5.26 ± 0.2	0.52 ± 0.03	30.1 ± 1.2
5	10.1 (CAPS) [0.04]	25.0 ± 0.1	6.30 ± 0.12	0.2 ± 0.5	0.0028 ± 0.008	0.2 ± 0.6

[a] Conditions as described in Experimental Section. [b] Error limits as deviation from the average of triplicate runs. [c] Error limits are standard deviation of linear plots of ln (^{18}O %) vs. time, three data points. [d] Only two points defining plot of ln (^{18}O %) vs. time.

Table V. Fractional Amounts of ^{18}O-Incorporated Amide Produced during the Hydrolyses of 3a,d and 5 in CD_3CN Containing 10–20 Vol % $H_2{}^{18}O$ as Determined by ^{13}C NMR Spectrometry[a,b]

		total material, %[a]		fractional material, %[b]	
compound	time, min	amide	acid	amide ^{16}O	amide ^{18}O
3a[c]	3	95.3	4.7	95.3	0
	15	68.0	32.0	60.2	7.8
	45	54.6	45.4	46.7	7.9
	90	34.0	66.0	26.0	8.0
3d[d]	45	68.0	32.0	63.4	4.6
	140	59.0	41.0	51.3	7.7
5[e]	2880	36	64	24.5	11.5

[a] Fractional % defined as (peak height given $^{13}C{=}O$ signal)/(Σ peak height all $^{13}C{=}O$ signals). For exact methodology, see Experimental Section d3. [b] Probable accuracy ±10% of value. [c] $\delta_{^{13}C=^{16}O}$ **3a** 192.326; $\delta_{^{13}C=^{18}O}$ **3a** 192.286; $\delta_{^{16}O-^{13}C-^{18}O}$ acid 169.45; $\delta_{^{18}O-^{13}C-^{18}O}$ acid 169.41. Conditions: 145 mg of **3a**; 450 μL of CD_3CN; 64 μL of $H_2{}^{18}O$; 30 °C. [d] $\delta_{^{13}C=^{16}O}$ **3d** 191.42; $\delta_{^{13}C=^{18}O}$ **3d** 191.37; $\delta_{^{16}O-^{13}C-^{18}O}$ acid 169.00; $\delta_{^{18}O-^{13}C-^{18}O}$ acid 168.96; $\delta_{^{16}O-^{13}C-^{16}O}$ acid 169.04. Conditions: 170 mg of **3d**; 450 μL of CD_3CN; 45 μL of $H_2{}^{18}O$; 30 °C. [e] $\delta_{^{13}C=^{16}O}$ **5** 189.01; $\delta_{^{13}C=^{18}O}$ **5** 188.97; $\delta_{^{16}O-^{13}C-^{18}O}$ (**10**) 176.56; $\delta_{^{18}O-^{13}C-^{18}O}$ (**10**) 176.54. Conditions: 150 mg of **5**; 500 μL of CD_3CN; 72 μL of $H_2{}^{18}O$; 30 °C.

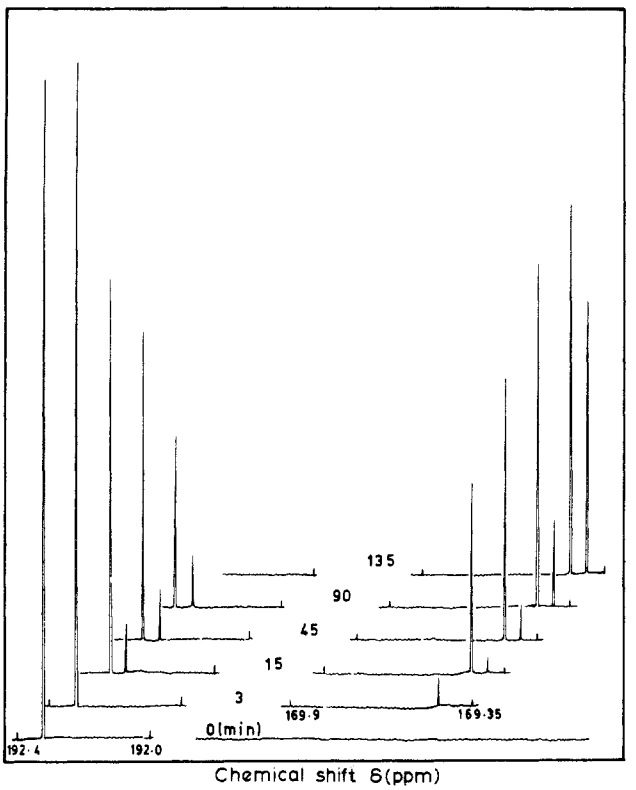

Figure 4. Graphical representation of the appearance of the $^{13}C{=}O$ NMR spectrum for **3a** as a function of time spent in a medium consisting of 450 μL of CD_3CN and 60 μL of $H_2{}^{18}O$; T = 30 °C. From low field to high field the origin of the peaks is ^{16}O amide, ^{18}O amide, ^{18}O–^{16}O acid, ^{18}O–^{18}O acid. Details given in Table V.

buffered aqueous solutions of the amides attain equilibrium pH values of ~4.7 after complete hydrolysis.) During the course of hydrolysis, the lowest field $^{13}C{=}^{16}O$ peak of the starting amide gives way to three additional $^{13}C{=}^{18}O$ resonances, one from ^{18}O-incorporated amide and one each from singly and doubly ^{18}O-labeled product acid. The appearance of the time-dependent ^{13}C NMR spectrum for **3a** is given in Figure 4. Control experiments with 50% ^{18}O-labeled **5** establish that the amide $^{13}C{=}^{18}O$ resonance is shifted 4 Hz upfield from the $^{13}C{=}^{16}O$ one and that the

Scheme II

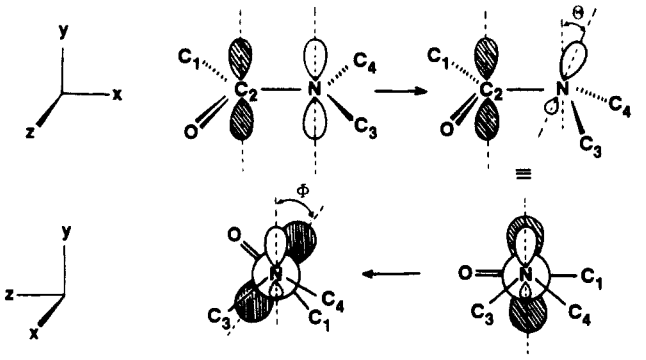

relative intensities are representative of the actual isotopic content.[22] Also, control experiments in which authentic double ^{16}O acid was added to the NMR mixture at the completion of hydrolysis demonstrate that a new resonance appears in the spectrum ~4 Hz downfield from the ^{16}O–^{13}C–^{18}O band. For **3a**, ~17% ^{18}O incorporation in the amide occurs at one hydrolysis half-life, a result which is very similar to that obtained from the quantitative reisolation experiments for **3a** detailed above. This would tend to indicate that the high CD_3CN content does not produce a major alteration of the exchange process and that the more qualitative results obtained in solutions containing acetonitrile need not be considered as atypical of the situation in H_2O.

Discussion

It is necessary at this point to consider the nature of the amide distortion in both **3** and **5**. Molecular models of **3** suggest that bridgehead N atom is tetrahedral with its sp^3 lone pair oriented coplanar with the C–O internuclear axis (i.e., orthogonal to the C=O π-bond). In **5**, X-ray crystallographic analysis[23] also indicates the N to be within 5° of a tetrahedral geometry and the relatively localized N lone pair is oriented 55–60° from coplanarity with the C–O internuclear axis. Thus, the distortion in these molecules is not simply that of twisting about the N—C=O bond.

The distortion can best be visualized as in Scheme II by considering a planar amide residing in the X–Z plane. Pyramidalization of the N produces a net tilt angle (θ) of the lone pair away from the y axis in the x direction. Coupled with that motion is a rotation of the C_1–C_2–O plane about the x axis to produce a twist angle (ϕ) of the p orbital on C away from coplanarity with the N lone pair. In terms of these motions, θ and ϕ are ~15–20° and 90°, respectively, for **3a–d** and ~15–20° and 30–35°, respectively, for **5**, the latter being experimentally observed by X-ray crystallography.[23] In actuality the asymmetry of the molecular structure in both **3** and **5** renders the π-faces of the C=O unit dissymmetric and hence it too should be somewhat pyramidalized or rehybridized from sp^2 toward sp^3.[24] Experimentally the C=O pyramidalization in **5** is

(22) As a control experiment 105 mg of detosylated **6d** (Scheme I) and 97 mg of **3d** (equimolar) in 500 μL of CD_3CN subjected to ^{13}C NMR analysis under the exact conditions used for the ^{18}O-exchange experiments (pulse delay 0.5 s, 1000 scans). Under these conditions, the relative intensities of the acid–amide $^{13}C{=}O$ signals was found to be 1.06:1.0. Considering the inherent inaccuracies of the measurements, the ^{13}C responses are therefore considered equivalent.

(23) (a) Skorey, K. I.; Somayaji, V.; Brown, R. S.; Ball, R. G., submitted for publication. (b) Brown, R. S.; Somayaji, V.; Skorey, K. I., submitted for publication. (c) Slebocka-Tilk, H.; Brown, R. S., submitted for publication.

Table VI. Second-Order Rate Constants (k_{OH^-}) for OH^--Catalyzed Hydrolyses of Some Amides at 25 °C in H_2O[a]

compound	k_{OH^-}, M^{-1} s^{-1}	ref
3-methyl-1-acetylbenzimidazolium	2×10^5	6e
3-methyl-1-acetyltetrahydrobenzimidazolium	1.0×10^5	6e
3-methyl-1-acetylimidazolium	1.5×10^5	6f
1-acetylbenzimidazole	4.67×10^2	6e
1-acetylimidazole	3.17×10^2	6c
3d	3.65×10^2	this work
3a	2.62×10^2	this work
3b	1.75×10^2	this work
3c	1.68×10^2	this work
5	6.0×10	this work
p-nitrophenyl acetate	1.49×10	*b*
N-acetylpyrrole	8.5[c]	3f
N-benzoylpyrrole	2.7	3f
α,α,α-trichloro-*N*-methylacetanilide	4.9×10^{-1}	3a
p-nitroacetanilide	2.2×10^{-3}	3b
1-phenylazetidin-2-one	1.27×10^{-3}	9b
1-phenyl-2-piperidone	2.0×10^{-5}	9b
p-methoxyacetanilide	8.19×10^{-6}	3c
p-chloroacetanilide	8.47×10^{-6}	3c
acetanilide	7.55×10^{-6}	3c
p-methylacetanilide	6.84×10^{-6}	3c

[a] Entries 1, 2, and 4 in 31.6% ethanol/H_2O. [b] Menger, F. M.; Portnoy, C. E. *J. Am. Chem. Soc.* **1968**, *90*, 1875–1878. [c] Refers to $k_1[OH^-]$ term in eq 1.

no more than 10°,[23] and we expect a reduced deformation for the C=O unit in **3** because it resides in a more symmetric environment.

Depending upon structure, amide resonance energy generally lies between 16 and 22 kcal/mol.[25] Values of θ and ϕ in excess of 0° will diminish the amide resonance since both motions tend to decrease the N:, C=O orbital overlap. The major difference between **3** and **5** stems not from changes in the tilt angle but in the torsional or twist angle. Assuming a cosine ϕ relationship for the N—C=O overlap[26] one can conclude that **5** is less torsionally strained than **3**. This is consistent with the lower $\nu_{C=O}$ for **5** than **3a**, 1705 cm^{-1} vs. 1755 cm^{-1}, respectively, both values exceeding $\nu_{C=O}$ for unstrained *N*-methylacetanilide (1665 cm^{-1}).[27]

At first glance, the most unusual aspect of the hydrolyses of **3** and **5** is the great reactivity in both acid and base

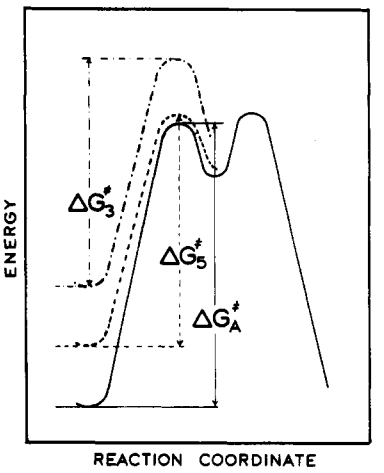

Figure 5. A stylized reaction coordinate/energy profile for OH^- attack on *N*-phenyl-2-piperidone (solid line, $\Delta G^{\ddagger}_A$), **3a** (·····, $\Delta G^{\ddagger}_3$) and **5** (- - -, $\Delta G^{\ddagger}_5$). $\Delta G^{\ddagger}_A - \Delta G^{\ddagger}_5 \simeq 9$ kcal/mol; $\Delta G^{\ddagger}_A - \Delta G^{\ddagger}_3 \simeq 10$ kcal/mol.

relative to "normal" anilides[3] and amides. Second-order rate constants for OH^--catalyzed hydrolysis for some selected amides and *p*-nitrophenyl acetate are given in Table VI. It may be concluded that **3** and **5** are among the most reactive neutral amides reported, comparing favorably with 1-acetylimidazole.

Several factors allow one to postulate with certainty the mechanism of base-induced hydrolysis of **3** and **5** as being akin to that given in eq 6. First, since no second-order

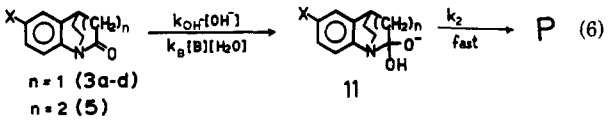

(6)

terms in $[OH^-]$ are seen in the hydrolysis kinetics and multiple ^{18}O incorporation into the product carboxylates is not observed, the first addition of OH^- must be rate limiting and essentially irreversible. This is supported by the FAB-determined composition of the carboxylates formed in 1 N $Na^{18}OH/H_2{}^{18}O$ from **3b**, **5** which show single ^{18}O incorporation. Reisolation of ^{18}O labeled **3a** from pH 9.8 CHES buffer gives 7.2 ± 0.4% ^{18}O exchange per $T_{1/2}$ of hydrolysis. However, at pH 9.8, under the conditions employed (0.02 M CHES, $k_{obsd} = 2.05 \times 10^{-2}$ s^{-1}) it can be calculated that the OH^--dependent term accounts for ~ 40% of the reaction. Hence, the probable sources of the ^{18}O depletion in reisolated amide **3a** at pH 9.8 are the residual H_2O and buffer terms.

The Hammett plot of the second-order rate constants for OH^- attack on **3a–d** against σ has a ρ of 0.72, indicative of an initial rate-limiting OH^- attack producing a transition state with increased − charge adjacent to the ring.

Finally, the observed general base catalysis seen at pH >8 for **3a–d** in base is consistent with assistance of H_2O attack on the C=O unit, the β-value of 0.8 ± 0.1 suggesting that this transition state is quite late with extensive proton transfer to the base. Although curvature in plots of k_{obsd} vs. [buffer] is sometimes seen in the base-catalyzed hydrolyses of activated acylacetanilides,[3j,1,11] none is seen for **3a–d**. Bicyclic **5** shows no general base catalysis of H_2O attack at pH >7 (HEPES and TRICENE buffers do show catalysis, but it is nucleophilic and will form the subject of a further study[23b]).

Our conclusion about the nature of the buffer catalysis for **3a–d** and that OH^- attack on **3a–d** and **5** is rate limiting and proceeds irreversibly contrasts the interpretation of Blackburn et al.,[7] who suggested on the basis of admittedly

(24) Mock, (Mock, W. L. *Bioorg. Chem.* **1975**, *4*, 270–278) has discussed torsional strain considerations and heavy atom rehybridization as it pertains to enzyme-catalyzed hydrolysis of peptides. In effect, torsional distortion of an amide must produce a C=O unit with disymmetric π-faces irrespective of any special structural features attributable to the bicyclic nature of **5**. Rehybridization of the C=O unit has the consequence of returning the axes of the (predominantly) p orbital on C and N lone pair into conjunction, thereby compensating to some extent the distortion energy.

(25) Winkler, F. K.; Dunitz, J. D. *J. Mol. Biol.* **1971**, *59*, 169–182.

(26) Streitweiser, A. *Molecular Orbital Theory for Organic Chemists*; Wiley: New York, 1961; pp 11–20.

(27) (a) The idea that $\nu_{C=O}$ is a measure of amide or ester hydrolytic reacticity is not new. For example Indelicato et al.[27b] have established a linear correlation between $\nu_{C=O}$ and log rate constant for base hydrolysis of a limited series of β-lactams. Also, for esters such as para-substituted phenyl acetates[27c] or methylbenzoates,[27c] good correlations of $\nu_{C=O}$ and various Hammett σ-values are observed. Since correlations between ester hydrolysis (log rate constants) and σ-values also exist,[27e] apparently $\nu_{C=O}$ and hydrolytic reactivity are correlated. It should be mentioned, however, that structural effects that influence $\nu_{C=O}$ will be predominantly ground state in nature, while the hydrolytic reactivity depends upon both the ground- and transition-state energies. Hence, correlations are to be expected only when the structural modifications in a series of compounds produces a regular change in both the ground and transition states. (b) Indelicato, J. M.; Norvilas, T. T.; Pfeiffer, R. R.; Wheeler, W. J.; Wilham, W. L. *J. Med. Chem.* **1974**, *17*, 523–527. (c) Cohen, L. A.; Takahashi, S. *J. Am. Chem. Soc.* **1973**, *95*, 443–448. (d) Laurence, C.; Berthelot, M. *J. Chem. Soc., Perkin Trans. 2* **1979**, 98–102. (e) Exner, O. In *Advances in Linear Free Energy Relationships*; Chapman, N. B., Shorter, J., Eds.; Plenum: London, 1972.

limited evidence for **3a**, that breakdown of the tetrahedral intermediate (**11** in eq 6) is rate limiting.

Given the above, it is possible to construct an energy profile for OH^--promoted hydrolysis. The lower trace in Figure 5 is a hypothetical reaction profile for OH^- attack on acetanilide or *N*-phenyl-2-piperidone. Since ^{18}O exchange is observed during hydrolysis of the former,[3c] the second barrier must be equal or slightly greater than that for reversal (i.e., $k_{-1} \geq k_3 + k_2[OH^-]$). Twisting and tilting the N electrons out of conjugation has the net effect of destabilizing the ground state of **3** by removing the amide resonance.

In **5** the combination of twisting and tilting distortions must also reduce the amide resonance energy, but it is difficult to quantitate the effect. Based on the observation that $\nu_{C=O}$ of **5** lies midway between $\nu_{C=O}$ of **3a** and *N*-methylacetanilide (NMA) it is tempting to place the ordering of amide resonance energy as NMA > **5** > **3a**.[27] Relative to *N*-phenyl-2-piperidone, the k_{OH^-} terms for **3a** and **5** are (1.3×10^7)- and (3×10^6)-fold larger which correspond the reductions in their respective activation energies to OH^- attack of 10 and 9 kcal/mol. The interesting speculation to be drawn from the above is that the apparently smaller distortion energy in **5** is more fully manifested in the transition state for base hydrolysis than is the larger distortion energy in **3a**.

For the same reasons that ground-state destabilization of **3** or **5** leads to a more rapid OH^- attack than on a normal anilide, the reverse of this step (k_{-1} in eq 1) must be decelerated since in that transition state there is no assistance by the N lone pair for ejection of the leaving group. This is schematically shown in Figure 5 as the higher barriers for reversion of **3** and **5**. It might be tempting to use Deslongchamps' arguments concerning stereoelectronic control[28] to speculate that the breakdown of the tetrahedral intermediate (T^-, eq 1) to proceed to product is unusually fast and that this is the reason for lack of ^{18}O exchange in base. As can be judged from **12** (N shaded), the two oxygen lone pairs can be ideally disposed antiperiplanar to the departing C–N bond but the N lone pair is oriented 60° relative to either C–O bond. The lack of

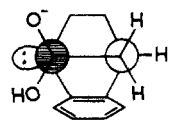

12

double ^{18}O incorporation in the base hydrolysis products of **3** and **5** is certainly consistent with a rapid breakdown of **12**, but the data do not require it to be *unusually* fast since the rate-limiting step is attack and the above arguments indicate that k_{-1} is retarded relative to a normal anilide. In actuality there is no reason to contend that the rate constant for breakdown of **12** should be greater than that of T^- of a normal anilide, since in the latter the lone pairs on oxygen can also attain the comparable configuration. [In fact, under acidic and neutral conditions, the breakdown of the intermediate to yield product cannot be unusually fast (vide infra).]

At neutrality, the mechanism of buffer-independent hydrolysis of **3** changes from OH^- attack to an apparent H_2O attack on the neutral form. The data at hand do not allow a clear distinction to be made between H_2O attack or the kinetically equivalent OH^- attack on the protonated form as was discussed by Blackburn et al.[7] However, the ^{18}O-exchange data observed for **3a** in pH 9.8 base suggest that the plateau region is best described as a water reaction. If OH^- attack on **3a** does not lead to ^{18}O exchange, it is difficult to envision how OH^- attack on **3a**-H^+ (which leads directly to an intermediate capable of breaking down to products with no proton transfers) could give ^{18}O exchange.

There is no apparent H_2O attack on neutral **5** so that the upper limit for that rate constant is $\sim 10^{-7}$ s^{-1} compared with 2×10^{-3} and 1.7×10^{-3} s^{-1} for the apparent attack of H_2O on **3a** and **3c**, respectively. While attack of the strong nucleophile OH^- on **3c** and **5** differs in rate by only a factor of 3, attack of imidazole, a weaker nucleophile, differs by 400-fold. That the latter process is ascribable to a nucleophilic role on both substrates is supported by the fact that 2-methylimidazole, (with similar basicity but possessing far greater steric hindrance for its nucleophilic attack than imidazole) shows a much reduced propensity to catalyze the decomposition of either **3c** or **5**.[23] No second-order kinetic terms in 2-methylimidazole are detected.

The pH–rate constant profiles for **3** show evidence of a kinetic pK_a for each substituent in the range of ~3.5–3.8. We believe this is ascribable to the N-protonated form,[18] the maximum rate constant for H_2O attack on it being 3.5–5 s^{-1}, nearly independent of substituent. However, a less straightforward but kinetically indistinguishable route involving H_2O attack on a highly reactive O-protonated form (**3**-OH^+) cannot explicity be ruled out. Given $pK_a^{3\text{-}OH^+} \simeq -8$[18] and $pK_a^{3\text{-}NH^+} = 4$ it can be seen that the ratio of O to N protonated **3** is $\sim 10^{-12}$, independent of pH. Now if **3**-OH^+ has a reactivity comparable to that of the most reactive oxocarbonium ions (lifetimes of 10^{-10}–10^{-13} s in H_2O),[21] then even though it is produced in miniscule concentration, its high reactivity could yield a net rate constant for H_2O attack on protonated **3** of $\sim 10^{-2}$–10 s^{-1}. Although the higher value seems appropriate for what is observed (Table I), we believe the rate data are more consistent with the expected H_2O reactivity with an N-protonated form. Williams[4f] has shown that certain *N*-acetyltrialkylammonium tetrafluoroborates hydrolyze at 25 °C with rate constants for H_2O attack on the order of 0.2 to 3.0×10^{-2} s^{-1} while Fersht and Jencks[29] have determined that attack of H_2O on *N*-acetylpyridinium proceeds with a pseudo-first-order rate constant of 6.9 s^{-1}. There is a dependency of the rate constants for hydrolysis of *N*-acylammonium ions[4f,29] on the basicity of the leaving group, and a β_{LG} value of −0.5 has been utilized in the above two studies. While it is not clear that compounds **3a–d** should follow the same dependency on leaving group as does the acylated quaternary ammonium or pyridinium species,[29b] it seems reasonable that the low $pK_{a_{LG}}$ of **3a–d** is responsible for the 10^2 increase in lability relative to the non-anilide materials studied by Williams.[4f]

The log k_{obsd} vs. pH plot for **5** (Figure 1) increases linearly until at least pH 0 (k_{obsd} = 59 s^{-1}; pH 0). Although rotation of the N̈—C=O dihedral angle from 90° (as in **3**) to smaller values is expected to produce a reduction in $pK_{a(NH^+)}$ from ~3.5, we believe the N-protonated species is not responsible for the much higher activity of **5** at low pH. Assuming that attack on **5** also adheres to a β_{LG} relationship, fully N-protonated **5** suffer H_2O attack at

(28) (a) Deslongchamps, P. *Stereoelectronic Effects in Organic Chemistry*; Pergamon: Oxford, 1983; and references therein. (b) See particularly pp 101–106 of the preceding reference for this point.

(29) (a) Fersht, A. R.; Jencks, W. P. *J. Am. Chem. Soc.* **1970**, *92*, 5432–5442. (b) Structurally, the *N*-acylpyridinium ions are quite unlike the quaternary *N*-acyl species, since in the former, considerable delocalization between the aromatic ring and *N*-acyl group is present. Hence the two series probably cannot be accurately correlated by a single Brønsted plot.[4f]

rates similar to those for N-protonated **3** since the pK_a values of the aniline leaving groups are similar and, once N-protonated, the electronic effects in the ground states are equal. The dihedral angle changes should also reduce the pK_a for O-protonated **5** from values of −1.2 to −2.59 which are commonly seen for substituted acetanilides[30] since resonance forms such as $>N^+=C<^{OH}$ are of reduced importance in **5**-H$^+$. However, for the same reason O-protonated **5** should be far more rapidly attacked by H_2O than normal O-protonated amides. Hence, while k_{H_2O} for attack on **5**-H$^+$ is 59 M^{-1} s^{-1} at 25 °C, the value for H_2O attack on **13**, **14**, and **15** are approximately (2–4) × 10^{-6}, (depending on the source of proton[31]), 3.8 × 10^{-8} [4f], and 8.1 × 10^{-7} M^{-1} s^{-1}, respectively. Analysis of the energetics of

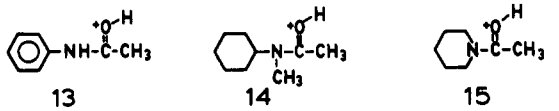

13 **14** **15**

the bimolecular rate constants for acid-catalyzed hydrolysis of O-protonated amides **5** and **13** reveals that the former's distortion results in a roughly 10 kcal/mol reduction in energy of activation. Using arguments similar to those above for the attack of OH^- on **5** and **3** relative to "normal" amides, it appears that the energy of distortion of amide **5** is (nearly) fully manifested in the transition state for acid-catalyzed hydrolysis as well. We feel that similar comparisons of the acid-catalyzed rates for **3a–d** with **5** and "normal" amides are tenuous since the sites of protonation are different.

Several lines of evidence indicate that in the neutral and acidic domain, the hydrolyses of **3** and **5** proceed through a reversibly formed intermediate. The most definitive support for this comes from the ^{18}O-incorporation studies. To explain the NMR hydrolysis data (Table V) and the ^{18}O exchange in amide recovered at pH <7 (Table IV) requires the intermediacy of a tetrahedral intermediate in which proton transfer, oxygen equilibrium, and reversal to starting material compete with product formation. The quantitative data in Table IV can be analyzed in terms of a simplified eq 7 wherein $k_{ex}/k_{hyd} = k_{-1}/2k_2$.[3e] Under the conditions given for **3a**, $k_2 \sim 1.7k_{-1}$, while for **5**, $k_2 \sim k_{-1}$.

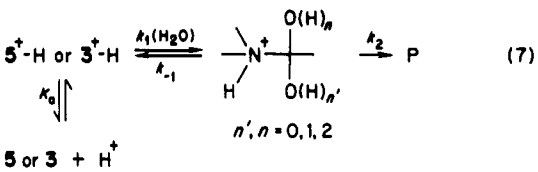

5-H or **3**-H ⇌ tetrahedral intermediate → P (7)

5 or **3** + H$^+$

$n', n = 0, 1, 2$

We have no additional kinetic evidence that pertains to the question of an intermediate in the acid hydrolysis of **5** since there is no indication of curvature in the acetate or formate buffer plots up to a concentration of 0.2 M. However, we have observed curvature in plots for the hydrolysis of **3c** with acetate buffers (Figure 2). Similar observations of curvature in the [buffer] plots for the base hydrolyses of trifluoromethyl acetanilides[3j,l,5b,10,11] were interpreted in terms of "superimposable buffer catalysis" wherein a change in rate-limiting step accompanies changes in [buffer]. From our data, it is not immediately clear whether the catalysis is general acid or general base. However, it might be anticipated that one can interpret the data of Figure 2 with acetate in terms of the simplified mechanism given in eq 7 which has an additional [buffer]-dependent term (k_2' [buffer]$_t$) leading from the intermediate to product. Assuming steady-state kinetics and rapid [H$^+$]-dependent preequilibrium formation of **3c**-H$^+$ gives the expression $k_{obsd} = k_1'(k_2 + k_2'[buffer]_t)/(k_{-1} + k_2 + k_2'[buffer]_t)$, where $k_1' = k_1[H^+]/(K_a^3 + [H^+])$. Nonlinear least-squares fitting of the k_{obsd} vs. total [acetate] data yields values of k_1', k_{-1}, k_2, and k_2' of 0.89, 0.38, 0.71 s^{-1}, and 5.26 M^{-1} s^{-1}, respectively, at pH 4.5, and 0.39, 0.62, 0.43 s^{-1}, and 3.85 M^{-1} s^{-1} at pH 5.1.[32] Although the fits in both cases are good (calculated vs. observed rate constants agreement within 4%), closer scrutiny reveals that the ratio of k_2/k_{-1} changes with pH. Since eq 7, as written, shows that this ratio is pH independent, one is forced to conclude that its present form is too simple.

All the above indicate that in the acid domain (and neutral for **3**) neither nucleophilic attack on the C=O unit nor product formation from the tetrahedral intermediate is entirely rate limiting. This is the probable source of the lack of correlation of the kinetic pK_a or k_1 and k_2 values (from Table I illustrated in Figure 2) with substituent effects. Bender and Thomas have demonstrated by indirect means that the attack step of OH^- on acetanilides correlates with σ^-, giving a ρ of +1.0, but the partitioning of the tetrahedral intermediate has a quite different substituent effect such that the overall dependence of k_{obsd} on substituent is very small.[3c]

The presence of a reversibly formed intermediate in the acid (and neutral) hydrolysis of **3** and **5** is deserving of further comment in the light of the Deslongchamps' stereoelectronic theory.[28] According to the theory, decomposition of a tetrahedral intermediate is facilitated in a particular direction when a lone pair of electrons on each of the remaining two groups is oriented antiperiplanar to the departing C–X bond. Clearly, under no circumstances can the N lone pair of **3** assist in the departure of an OH or $^+OH_2$ group. Examination of molecular models of the tetrahedral intermediate of **5** indicates that the N lone pair is ~30° out of a syn periplanar orientation with one C–O bond, and essentially orthogonal to the other. Since the relative orientations of the oxygens can be interchanged by a ring flip one might invoke some conjugation of the N lone pair (even though not optimally oriented anti periplanar but skewed syn) in assisting oxygen departure and therefore ^{18}O exchange in **5**. However, these arguments cannot be invoked to explain the substantial exchange observed for **3** (Tables IV and V).

As illustrated in **16**, the two oxygens (assuming rapid proton transfer and/or C–O bond rotation) can have lone pairs (shaded) ideally disposed anti periplanar to the departing C–N bond regardless of whether **16** arose from **3** or **5**. Two other features of **16** bias the cleavage of the

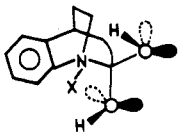

16 X = :, H$^+$

C-N bond even further. First, the departing electrons are conjugated with the aromatic ring, which should make the aniline a better leaving group than an amino group,[10b,33,34] and second, that transition state should benefit by relieving some strain inherent in the bicyclic system.

(30) Giffney, C. J.; O'Connor, C. J. *J. Chem. Soc., Perkin Trans. 2* **1975**, 706–712.
(31) Barnett, J. W.; O'Connor, C. J. *J. Chem. Soc., Perkin Trans. 2* **1973**, 220–222.
(32) An equally good plot is obtained if either the acidic or basic form of the buffer is used.
(33) Ewing, S. P.; Lockshon, D.; Jencks, W. P. *J. Am. Chem. Soc.* **1980**, *102*, 3072–3084.
(34) (a) McClelland, R. A.; Patel, G. *J. Am. Chem. Soc.* **1981**, *103*, 6908–6911 and references therein. (b) Gravitz, N.; Jencks, W. P. *Ibid.* **1974**, *96*, 499–506. (c) McClelland, R. A. *Ibid.* **1978**, *100*, 1844–1849.

In spite of the "loading" to favor C–N cleavage and disfavor C–O cleavage, the tetrahedral intermediates do not undergo an unusually preferential breakdown to products, even when the nitrogen is protonated. This is clearly contrary to the Deslongchamps' theory since the tetrahedral intermediates are never expected to revert back to (exchanged) starting materials.[28b] Recently Perrin and Arrhenius have critically examined much of the evidence upon which the stereoelectronic theory is based and found it to be ambiguous.[35] At least two examples, one in acetal hydrolysis[36a] and another amide hemiacetal cleavage,[36b] have been reported which must proceed without stereoelectronic control.

Rationalizing the exchange observed in the acidic range requires due consideration of both the bicyclic structure and the relative leaving group abilities of a $CN^+(H)<$ group with two O antiperiplanar lone pairs, or a $C-O^+H_2$ unit with one O antiperiplanar lone pair to assist departure. The OH of **16**, though less basic ($pK_a \sim -4$[19b]) which makes it less likely to protonate than N ($pK_a \sim 4$[37]), becomes a much better leaving group when protonated or partially so,[34] and hence C–O cleavage can compete with C–N cleavage in acid. In a given situation, whether both modes of cleavage compete is difficult to predict since there is a subtle balance of effects. For example, in **17** (Ar = C_6H_5) the $(C-O/C-N)_{acid}$ cleavage ratio is nearly unity while in **18** C–N cleavage is exclusively observed.[34] Presumably the reduction in pK_a of the anilinium group in **18** (which in principle would disfavor C–N cleavage since less N-protonated material is present) is more than compensated for by the increased leaving group ability of an anilinium vs. ammonium group.

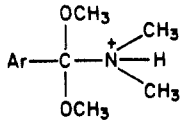

17[34c]

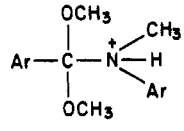

18[34a]

Conclusions and Speculations

An attractive hypothesis for enzyme catalysis is that the introduction of strain in the substrate, enzyme, or both on formation of the E·S complex plays an important part in bringing about the observed rate accelerations.[2] In several instances, better substrates for a specific enzyme lead to larger k_{cat} terms, but within certain limits, this occurs with little change in the Michaelis constant. For example, Hofstee has shown that the hydrolysis rate of substituted phenyl esters ($CH_3(CH_2)_nCO_2$ $ArCO_2^-$) catalyzed by liver esterase or chymotrypsin increases with increasing values of n, which apparently leads to a larger number of productive E·S contacts with a concomitant induction of strain.[38] Similarly, pepsin-catalyzed hydrolyses of some tri- and tetrapeptides show a variation of 10^3 in k_{cat}, but K_M varies randomly by only a factor of 4.[39] Analogous findings with elastase catalysis of peptide hydrolysis were interpreted in terms of distortion of the scissile amide C=O toward the transition-state geometry.[40] Although this hypothesis is difficult to test by crystallographic (or other) means, pyramidal distortion of the C=O unit of a reactive peptide has been reported in structures of various forms of trypsin with pancreatic trypsin inhibitor.[41] However, Read et al.[42] have found no C=O distortion in the refined structures of *streptomycesgriseus protease B* inhibited with turkey ovomucoid inhibitor.

One would like to have some idea whether an amide with a distorted N—C=O unit can hydrolyze rapidly enough to be considered as a plausible candidate for that same proposal in the enzyme-mediated hydrolysis of a peptide. Also, one would like to know whether the more significant acceleration arises from twisting the N lone pair out of conjugation, the tilting which is achieved on N pyramidalization, or some combination of the two motions. The present study (and the one reported by Blackburn et al.[7] for **3a**) has shown that these anilides hydrolyze 10^6–10^7-fold more rapidly in both acid and base than do their nondistorted counterparts. This is attributable to an acceleration of nucleophilic attack rather than an enhanced rate of breakdown of the tetrahedral intermediates.

Anilides **3a** and **5** differ in reactivity toward OH^- by only a factor of ~5–6 even though the latter is twisted much less (θ_5 = 30–35° vs. θ_{3a} = 90°). This may suggest that the major reduction in the transition state barrier is realized after a relatively small twisting distortion. Additionally, it must be recalled in both cases the N is pyramidalized toward sp^3. That rehybridization, even in the absence of twisting leads to a significant reduction in the $\ddot{N}C=O$ interaction.[23c]

An important facet of the above study centers around the ^{18}O-exchange results observed for **3** and **5**. Contrary to what is observed for substituted acetanilides,[3c] neither **3** nor **5** undergo ^{18}O exchange when attacked by OH^-. Clearly for the latter, the rate-limiting step is attack, and the tetrahedral intermediate is formed irreversibly. In acid, extensive ^{18}O exchange is observed for both **3** and **5**, whereas normal acetanilides show no ^{18}O exchange.[3] The extent to which this is attributable to the unique bicyclic structures of **3** and **5**, the reaction conditions, or the presence of buffers is at present unknown. However, this raises the possibility that oxygen equilibration and reversal from the tetrahedral intermediates formed during acid-catalyzed amide hydrolysis may be a far more prominent occurance than is currently believed.

Acknowledgment. We gratefully acknowledge the financial assistance from the Natural Sciences and Engineering Research Council of Canada and the University of Alberta; in particular we acknowledge receipt of a grant from the Central Research Fund of the University of Alberta and discussions with Dr. J. P. Street. In addition, we acknowledge the helpful advice of the referees and Professor Charles L. Perrin (University of California, San Diego).

Registry No. **3a**, 76059-52-4; **3b**, 102586-85-6; **3c**, 102586-86-7; **3d**, 102586-87-8; **5**, 102586-88-9; **6**, 102586-89-0; **7**, 102586-91-4; **8**, 102586-92-5; **9**, 67752-46-9; **10**, 102586-93-6; *N*-(*p*-toluenesulfonyl)-1,2,3,4-tetrahydroquinoline-4-acetyl chloride, 102586-90-3; deuterium, 7782-39-0.

Supplementary Material Available: Kinetics data and ^{18}O-exchange data (mass spectrometric intensities) (6 pages). Ordering information is given on any current masthead page.

(35) Perrin, C. L.; Arrhenius, G. M. L. *J. Am. Chem. Soc.* **1982**, *104*, 2839–2842.

(36) (a) Chandrasekhar, S.; Kirby, A. J. *J. Chem. Soc., Chem. Commun.* **1978**, 171–172. (b) Deslongchamps, P.; Dubé, S.; Lebreux, C.; Pattersen, D. R.; Taillefer, R. J. *Can. J. Chem.* **1975**, *53*, 2791–2807.

(37) An estimate of the pK_a of **16**-H^+ can be made by utilizing a drop of ~3.7 pK units in passing from $RCH_2N^+H(CH_3)_2$ (i.e., 9.86 to 6.10) according to the procedure of Guthrie.[19b] Since the pK_a of benzoquinuclidine is 7.79,[20] the pK_a of **16**-H^+ is estimated to be 4.0.

(38) (a) Hofstee, B. H. J. *Biochem. Biophys. Acta* **1957**, *24*, 211–213; (b) **1959**, *32*, 182–188.

(39) (a) Inouye, K.; Fruton, J. S., *Biochemistry* **1967**, *6*, 1765–1777. (b) Sachdev, G. P.; Fruton, J. S. *Ibid.* **1970**, *9*, 4465–4470.

(40) (a) Thompson, R. C. *Biochemistry* **1973**, *12*, 47–57; (b) **1974**, *13*, 5495–5501. (c) Thompson, R. C.; Blout, E. R. *Ibid.* **1973**, *12*, 57–65.

(41) Huber, R.; Bode, W. *Acc. Chem. Res.* **1978**, *11*, 114–122.

(42) Read, R. J.; Fujinaga, M.; Sielecki, A. R.; James, M. N. G. *Biochemistry* **1983**, *22*, 4420–4433.